

Preliminary Examination

Joe Camilleri

Virginia Tech

prelim exam

Dirac equation and charge conjugation

$$\mathcal{L} = \frac{i}{2} [\bar{\psi} \gamma^\mu (\partial_\mu \psi) - (\partial_\mu \bar{\psi}) \gamma^\mu \psi] - \textcircled{m\bar{\psi}\psi}$$

$$(i\not{\partial} - m)\psi = 0$$

$$\psi = \begin{pmatrix} \varphi \\ \chi \end{pmatrix}$$

The Quantum Theory of the Electron.

By P. A. M. DIRAC, St. John's College, Cambridge.

(Communicated by R. H. Fowler, F.R.S.—Received January 2, 1928.)

The new quantum mechanics, when applied to the problem of the structure of the atom with point-charge electrons, does not give results in agreement with experiment. The discrepancies consist of "duplexity" phenomena, the observed number of stationary states for an electron in an atom being twice the number given by the theory. To meet the difficulty, Goudsmit and Uhlenbeck have introduced the idea of an electron with a spin angular momentum of half a quantum and a magnetic moment of one Bohr magneton. This model for the electron has been fitted into the new mechanics by Pauli,* and Darwin,† working with an equivalent theory, has shown that it gives results in agreement

$$e^- \longleftrightarrow e^+$$

$$\hat{\psi} \rightarrow \hat{\psi}^C = C \gamma^0 \hat{\psi}^*$$

$$C = \begin{pmatrix} i\sigma_2 & 0 \\ 0 & -i\sigma_2 \end{pmatrix}$$

Majorana fermions and neutrinos

- Majorana fermions can be seen as solutions to the Dirac equation with an extra constraint
- $\psi = \psi^C$
- implies these fermions are **chargeless**, and their **own anti-particles**

The left and right handed components of the spinor are no longer independent

$$\hat{\psi} = \begin{pmatrix} \hat{\varphi} \\ -i\sigma_2(\varphi^\dagger)^T \end{pmatrix} = \begin{pmatrix} \hat{\psi}_L \\ \hat{\psi}_R \end{pmatrix}$$

mass terms:

$$\begin{aligned} & \left(\overline{\hat{\psi}}^C_L \hat{\psi}_L + \overline{\hat{\psi}}_L \hat{\psi}_L^C \right)_{Majorana} \\ & \left(\overline{\hat{\psi}}_L \hat{\psi}_R + \overline{\hat{\psi}}_R \hat{\psi}_L \right)_{Dirac} \end{aligned}$$

$$\begin{aligned} \hat{\psi}(x_\mu) = & \int \frac{d^3\bar{k}}{(2\pi)^3 2\omega_k} \sum_s \\ & \left[\hat{b}(\bar{k}, s) u(\bar{k}, s) e^{-ik^\mu x_\mu} \right. \\ & \left. + \hat{b}^\dagger(\bar{k}, s) v(\bar{k}, s) e^{+ik^\mu x_\mu} \right] \end{aligned}$$

why is Dirac/Majorana nature still unknown?

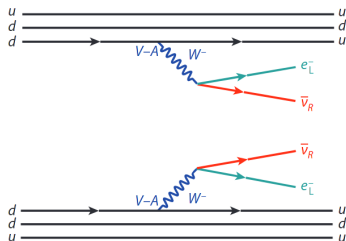
- Both types of fermions are compatible with observed features of neutrinos, *including* neutrino oscillations. Majorana neutrinos and their anti-matter partners are only distinguishable by their chirality.
- In the ultra-relativistic limit, helicity and chirality are equivalent e.g. we can never boost into a frame where a neutrino has right handed helicity.
- V-A interaction has left-handed projection operator, so we only observe β -decay that is also consistent with Dirac neutrinos that respect lepton number conservation (an accidental symmetry).

$$\mathcal{L}_{cc} = -\frac{g}{\sqrt{2}} \left[\bar{e} \gamma^\mu \left(\frac{1 - \gamma_5}{2} \right) \nu W_\mu^- + \bar{\nu} \gamma^\mu \left(\frac{1 - \gamma_5}{2} \right) e W_\mu^+ \right]$$

$$\hat{\nu} = \int \frac{d^3 \bar{k}}{(2\pi)^3 2\omega_k} \sum_s \left[\hat{b}(\bar{k}, s) u(\bar{k}, s) e^{-ikx} + \hat{b}^\dagger(\bar{k}, s) v(\bar{k}, s) e^{+ikx} \right]$$

SM and BSM double-beta decay

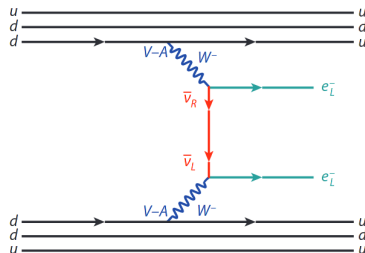
$2\nu\beta\beta$: the neutrinos are Dirac fermions, and have distinct anti-particles $\nu, \bar{\nu}$



extremely rare process, observed in direct detection experiments

$$T_{1/2}^{2\nu\beta\beta} \sim 10^{19} - 10^{24} \text{ yr}$$

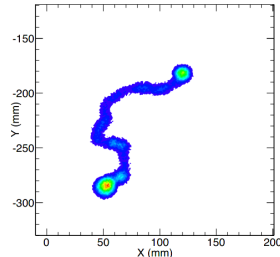
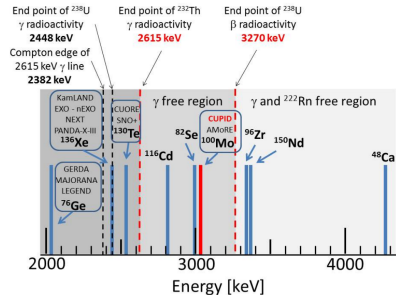
$0\nu\beta\beta$: the neutrinos are Majorana fermions and are absorbed as virtual particles



Never before observed in any experiment: $T_{1/2}^{0\nu\beta\beta} > 10^{26} \text{ yr}$ (Lepton number violation)

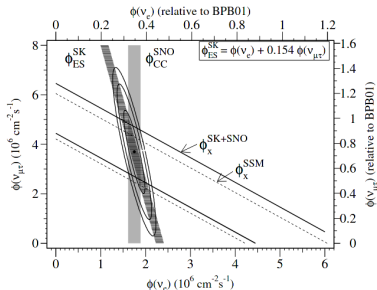
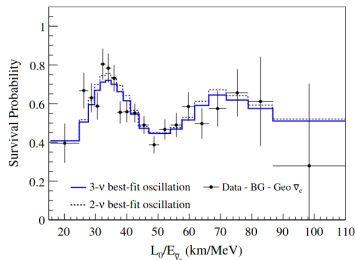
experimental signature and detection

- mono-energetic peak with 2 electrons leaving the reaction.
- tomography of electron tracks can help reduced backgrounds, except for the $2\nu\beta\beta$ irreducible background
- experimental goal is to measure $T_{1/2}^{0\nu\beta\beta}$ to constrain the effective neutrino mass $m_{\beta\beta}$.
- this measurement complements measurements of Σ and m_{β} from cosmology and kinematic experiments, respectively.



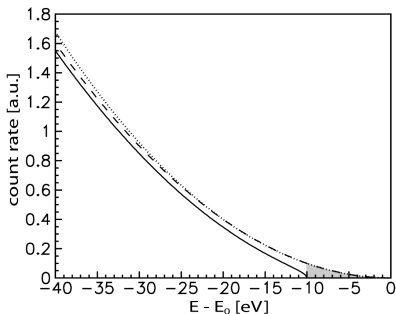
neutrino mass and oscillations

- Homestake Mine and the solar neutrino anomaly
 $^{37}\text{Cl} + \nu_e \rightarrow ^{37}\text{Ar} + e^-$
 observes factor of 3 discrepancy in ν_e flux.
- Sudbury Neutrino Observatory (SNO) measures total neutrino flux: ν_μ, ν_τ account for ν_e deficit.
- KAMLAND, a reactor neutrino experiment shows survival probability of electron neutrinos
 $P = 1 - \sin^2(2\theta)\sin^2(\Delta m^2 L/4E)$



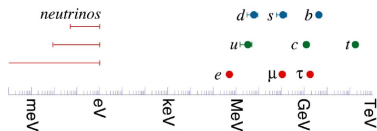
neutrino mass and the β -spectrum

- Tritium (3H) is a viable isotope for directly probing the neutrino mass - low Q value (decays in region $E_0 - E$ scale with $(E_0 - E)^3/Q^3$ and short-life to reduce line broadening.....?
- Measure deviation from the mass-less spectrum's linearity at large energies.
- This method is most-direct and model independent probe of the neutrino's mass. Constructing a sensitive experiment is very challenging (KATRIN may be last of its kind)



mass scale

- Physicists believed neutrinos to be massless for decades, due to Standard Model predictions (Higgs mechanism for leptons) and experimental data
- Neutrinos are orders of magnitude lighter than any other fundamental particle. This in addition to them being chargeless, makes it hard to measure their presence in experiments.
- The common model for describing BSM neutrino mass states is the light-neutrino mixing model (3 mass eigenstates)



neutrino mixing

A given flavor eigenstate is a linear combination of mass eigenstates (PMNS-matrix)

$$\begin{bmatrix} \nu_e \\ \nu_\mu \\ \nu_\tau \end{bmatrix} = U \begin{bmatrix} \nu_1 \\ \nu_2 \\ \nu_3 \end{bmatrix}$$

parameters: angles
 $\theta_{12}, \theta_{13}, \theta_{23}$ CP-violating
phases $\delta_{CP}, \alpha_1, \alpha_2$, and
neutrino masses m_1, m_2, m_3

$$U = \begin{pmatrix} c_{12}c_{13} & s_{12}c_{13} & s_{13}e^{-i\delta_{CP}} \\ -s_{12}c_{23} - c_{12}s_{23}s_{13}e^{i\delta_{CP}} & c_{12}c_{23} - s_{12}s_{23}s_{13}e^{i\delta_{CP}} & s_{23}c_{13} \\ s_{12}s_{23} - c_{12}c_{23}s_{13}e^{i\delta_{CP}} & -c_{12}s_{23} - s_{12}c_{23}s_{13}e^{i\delta_{CP}} & c_{23}c_{13} \end{pmatrix} \\ \times \begin{pmatrix} e^{i\alpha_1/2} & 0 & 0 \\ 0 & e^{i\alpha_2/2} & 0 \\ 0 & 0 & 1 \end{pmatrix}$$

mass hierarchy

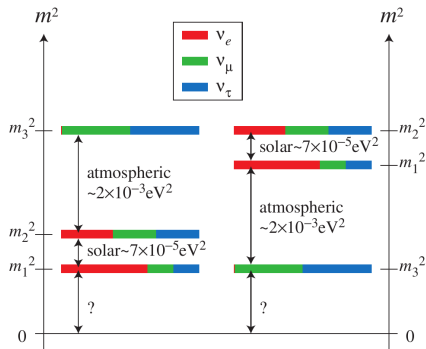
Neutrino oscillation experiments are sensitive to $\Delta m_{ij}^2 = m_i^2 - m_j^2$. This, coupled with the neutrinos' very small mass scale, leads to ambiguity in their ordering.

normal ordering

$$\Rightarrow m_3^2 > m_2^2 > m_1^2$$

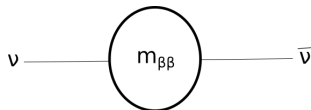
inverted ordering

$$\Rightarrow m_2^2 > m_1^2 > m_3^2$$

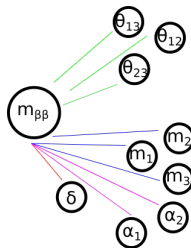


effective Majorana neutrino mass

$$m_{\beta\beta} = \sum |U_{ei}|^2 v_i|$$



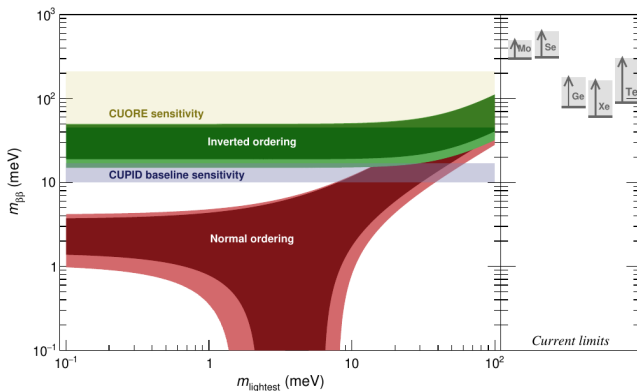
$$m_{\beta\beta} \bar{\psi}\psi$$



zero neutrino half-life

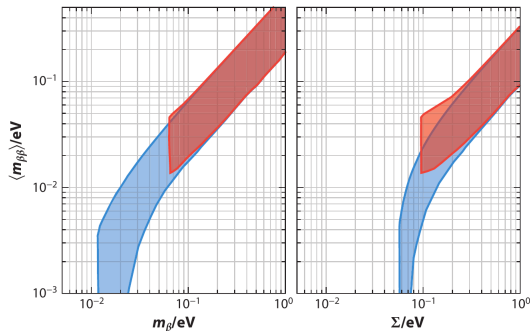
$$T_{1/2}^{0\nu\beta\beta} = (G|\mathcal{M}|^2\langle m_{\beta\beta}\rangle)^{-1}$$

$$\langle m_{\beta\beta}\rangle = \Sigma|U_{ej}^2m_j|$$



complementary limits

- Limits on the effective $0\nu\beta\beta$ half-life are also constrained by kinematic and cosmological searches
- $m_\beta = \sqrt{U_{ei}^2 m_i^2}$ and $\Sigma = m_1 + m_2 + m_3$
- $m_\beta < 1.1\text{eV}$
 $\Sigma < 0.3\text{eV}$



inverted normal

designing a direct-detection experiment

Isotope	$Q_{\beta\beta}$ (keV)	I.A. (%)	$G^{0\nu}$	$H^{0\nu}$
^{48}Ca	4272	0.187	24.81	826.2
^{76}Ge	2039	7.8	2.36	49.6
^{82}Se	2995	8.73	10.16	198.1
^{96}Zr	3350	2.8	20.58	342.7
^{100}Mo	3034	9.63	15.92	254.5
^{110}Pd	2018	11.72	4.82	70.0
^{116}Cd	2814	7.49	16.70	230.1
^{124}Sn	2287	5.79	9.04	116.5
^{128}Te	866	31.69	0.59	7.4
^{130}Te	2527	33.8	14.22	174.8
^{136}Xe	2458	8.9	14.58	171.4
^{148}Nd	1929	5.76	10.10	109.1
^{150}Nd	3371	5.64	63.03	671.7
^{154}Sm	1215	22.7	3.02	31.3
^{160}Gd	1730	21.86	9.56	95.5
^{198}Pt	1047	7.2	7.56	61.0

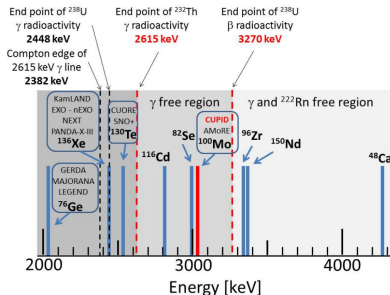
$$T_{1/2}^{0\nu\beta\beta} = (G|\mathcal{M}|^2\langle m_{\beta\beta} \rangle)^{-1}$$

$$F_{0\nu} = \ln(2) N_{\beta\beta} \epsilon \frac{t}{n_{bkg}}$$

$$F_{0\nu} = \ln(2) \times \frac{N_A}{W} \left[a \epsilon \sqrt{\frac{Mt}{b\Delta}} \right]$$

backgrounds

- Primordial radioisotopes: ^{238}U and ^{232}Th generate chain of β, γ near $Q_{\beta\beta}$.
- ^{222}Rn can exist in gaseous state produces $\beta + \gamma$ impinging on $Q_{\beta\beta}$
- ^{208}Tl emits γ at 2615 keV, affecting a number of candidate source isotopes.
- the intrinsically irreducible background $2\nu\beta\beta$: $\Gamma_{2\nu\beta\beta}$ is negligible in some isotopes (^{130}Te), but not others (^{100}Mo)
- muons enter the backgrounds in a number of ways: prompt signal + long-lived isotope activation + neutron production



Next Generation $0\nu\beta\beta$ experiments

goal: probe $0\nu\beta\beta$ to a half life of 10^{28} years

requirement: $B.I. =$

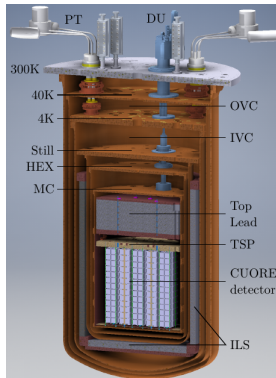
$0.1 \text{ counts} / (\text{FWHM} \cdot \text{tonne} \cdot \text{year})$

CUPID conservative goal: $B.I. =$

$0.5 \text{ counts} / (\text{FWHM} \cdot \text{tonne} \cdot \text{year})$

CUORE experiment

- Array of 988 TeO_2 bolometers instrumented with NTD sensors.
- CUORE cryostat maintains about 200kg of ^{130}Te around 10mK.
- current limit on $0\nu\beta\beta$ in ^{130}Te :
 $T_{1/2}^{0\nu} > 3.2 \cdot 10^{25} \text{yr}$

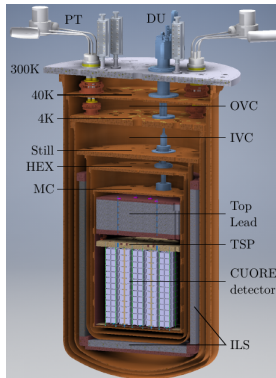


Cuore

cryostat is a dilution refrigerator that
 cools 750kg of mass to 10mK

CUORE backgrounds

- irreducible $2\nu\beta\beta$ rate is negligible relative to
- CUORE cryostat maintains about 200kg of ^{130}Te around 10mK.
- current background index is $10^{-2} \text{ counts}/(\text{keV} \cdot \text{kg} \cdot \text{yr})$

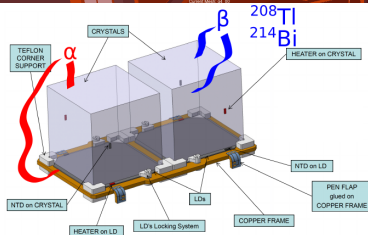
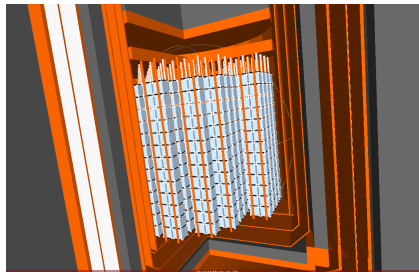


Cuore

cryostat is a dilution refrigerator that
cools 750kg of mass to 10mK

CUPID experiment

- Proposed array of 1596 Li_2MoO_4 to be deployed in the CUORE cryostat
- aims to address dominant background of α -particles in CUORE.
- capitalize on processes (CR6) and technology (cryostat and calibration) developed for CUORE
- current research is to address new backgrounds introduced with new source material to improve BI
 $\sim 10^{-4} \text{ counts}/(\text{keV} \cdot \text{kg} \cdot \text{year})$

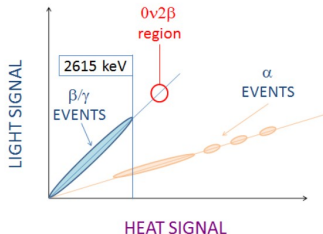
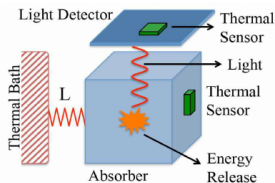


Lithium molybdate

- Li_2MoO_4 crystals allow for discrimination of α backgrounds from $\beta\beta$ events ($Q=3034\text{keV}$) via thermal + scintillation signals.
- relatively high isotopic abundance of ^{100}Mo (10%)
- enrichment above 95% already demonstrated in CUPID-Mo¹.

¹arxiv.org/abs/1909.02994.

Scintillating Bolometer



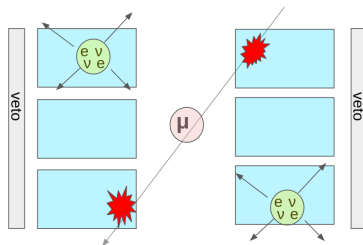
$2\nu\beta\beta$ events and muons

- The rate of $2\nu\beta\beta$ events is not negligible² in the CUPID array
- Minimizing the distance cut helps avoid mis-labelling random $2\nu\beta\beta$ coincidences as multiplicity 2.
- Assuming a simple muon veto geometry, increasing the distance cut rejects more muon events.

$$T_{1/2}^{2\nu\beta\beta}(^{100}\text{Mo}) = 7.1 * 10^{18} \text{ yr}$$

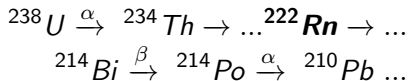
$$\rightarrow \text{single crystal rate} \sim 3 \text{ mHz}$$

$$T_{1/2}^{2\nu\beta\beta} \sim 10^{19} - 10^{24} \text{ yr}$$

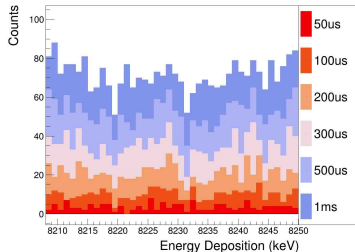
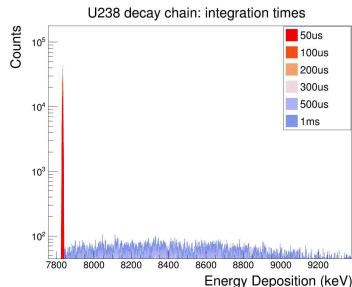


²arxiv.org/abs/1912.07272.

Integration time in the CUPID array

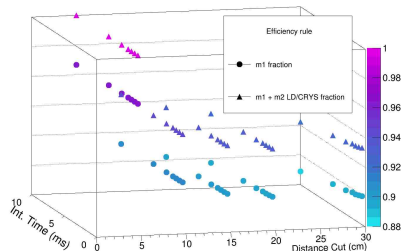
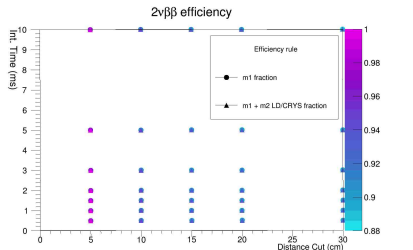


- 100,000 Uranium-238 events (full chain)
- $T_{1/2} ^{214}\text{Po} \sim 160\mu\text{s}$
- $T_{1/2} ^{214}\text{Bi} \sim 20 \text{ minutes}$



$2\nu\beta\beta$ tagging simulation

- 40 million events generated in crystal volume.
- expect $\sim 90\%$ efficiency for $2\nu\beta\beta$ tagging, when using approximate CUORE parameters
- larger distance cut causes more random coincidences and more variation with integration time
- bremsstrahlung, escape, random coincidences are primary contributors

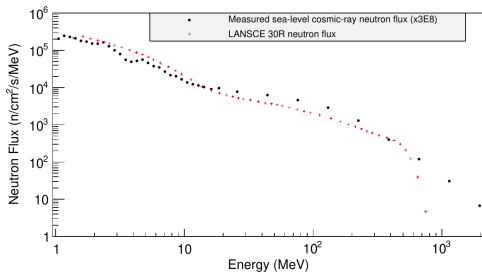


spallation in ^{100}Mo

$$\sigma = \sigma_0 f(A) f(E) e^{-P\Delta A} \times \exp(-R|Z| - SA + TA^2 + UA^3 |^\nu \Omega \eta \xi)$$

- semi-empirical cross section formula
- at LANL, a beam bombarding protons on a tungsten target mimics the cosmic ray spectrum.
- $3 \cdot 10^8$ scaling in flux \Rightarrow 2 days of beam time equates to 1 million years of sea-level exposure.

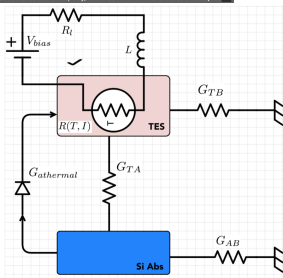
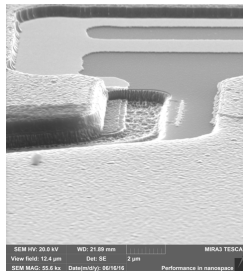
\Rightarrow currently implementing spectrum for parasitic neutron simulation and are proposing to perform a measurement at LANL neutron beam.



product	Q(MeV)	$T_{1/2}$	A_{initial} (Bq)	$A_{1\text{yr}}$ (Bq)
^{56}Co	4.5	77 d	$5.1 \cdot 10^{-8}$	$2.1 \cdot 10^{-9}$
^{88}Y	3.6	106 d	$2.2 \cdot 10^{-5}$	$2 \cdot 10^{-6}$
^{26}Al	4	$7 \cdot 10^5 \text{ yr}$	$2.1 \cdot 10^{-8}$	$2.1 \cdot 10^{-8}$
^{48}V	4	16 d	$4.1 \cdot 10^{-8}$	$5.4 \cdot 10^{-15}$
^{96}Nb	3.2	1 d	$4.7 \cdot 10^{-3}$	≈ 0

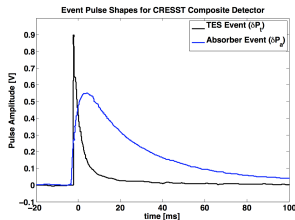
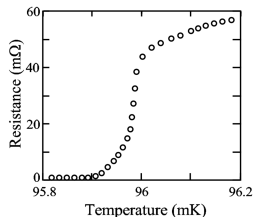
transition edge sensors

- Motivation is two-fold: good energy resolution improves efficiency in the region of interest + higher bandwidth operation enables $2\nu\beta\beta$ suppression
- superconducting films biased in transition region have exceptional sensitivity
 $\frac{\alpha_{TES}}{\alpha_{semi}} \sim 100$ and bandwidth
 $\omega \sim G/C$
- voltage biased, electrothermal-feedback TES solve bias and thermal-runaway, but also requires the implementation of SQUID's as readout devices.



challenges applying to $0\nu\beta\beta$

- Require good coverage for light detector application
- sensor-absorber bandwidth mismatch is limiting factor in energy resolution
- low- T_c devices are also necessary because of operating temperature of the detector itself.
- TES dynamic range is limited by the width of the transition $\mathcal{O}(mK)$. $Q_{\beta\beta} \sim MeV$



Robeson 1 low-temperature laboratory

